doi:10.1093/brain/aww167 BRAIN 2016: 139; 2431–2440 | 2431

BRAIN
A JOURNAL OF NEUROLOGY

The superficial white matter in temporal lobe epilepsy: a key link between structural and functional network disruptions

Min Liu, Boris C. Bernhardt, Seok-Jun Hong, Benoit Caldairou, Andrea Bernasconi and Neda Bernasconi

Drug-resistant temporal lobe epilepsy is increasingly recognized as a system-level disorder affecting the structure and function of large-scale grey matter networks. While diffusion magnetic resonance imaging studies have demonstrated deep fibre tract alterations, the superficial white matter immediately below the cortex has so far been neglected despite its proximity to neocortical regions and key role in maintaining cortico-cortical connectivity. Using multi-modal 3 T magnetic resonance imaging, we mapped the topography of superficial white matter diffusion alterations in 61 consecutive temporal lobe epilepsy patients relative to 38 healthy controls and studied the relationship to large-scale structural as well as functional networks. Our approach continuously sampled mean diffusivity and fractional anisotropy along surfaces running 2 mm below the cortex. Multivariate statistics mapped superficial white matter diffusion anomalies in patients relative to controls, while correlation and mediation analyses evaluated their relationship to structural (cortical thickness, mesiotemporal volumetry) and functional parameters (resting state functional magnetic resonance imaging amplitude) and clinical variables. Patients presented with overlapping anomalies in mean diffusivity and anisotropy, particularly in ipsilateral temporo-limbic regions. Diffusion anomalies did not relate to cortical thinning; conversely, they mediated large-scale functional amplitude decreases in patients relative to controls in default mode hub regions (i.e. anterior and posterior midline regions, lateral temporo-parietal cortices), and were themselves mediated by hippocampal atrophy. With respect to clinical variables, we observed more marked diffusion anomalies in patients with a history of febrile convulsions and those with longer disease duration. Similarly, more marked diffusion alterations were associated with seizure-free outcome. Bootstrap analyses indicated high reproducibility of our findings, suggesting generalizability. The temporo-limbic distribution of superficial white matter anomalies, together with the mediation-level findings, suggests that this so far neglected region serves a key link between the hippocampal atrophy and large-scale default mode network alterations in temporal lobe epilepsy.

Neuroimaging of Epilepsy Laboratory, McConnell Brain Imaging Center, Montreal Neurological Institute and Hospital, McGill University, Montreal, Quebec, Canada

Correspondence to: Neda Bernasconi, MD PhD,
Montreal Neurological Institute (WB-322),
3801 University Street, Montreal, Quebec,
Canada H3A 2B4
E-mail: neda@bic.mni.mcgill.ca

Keywords: multimodal MRI; superficial white matter; functional network; mediation analysis

Abbreviations: ALFF = amplitude of low-frequency functional fluctuations; ILAE = International League Against Epilepsy; TLE = temporal lobe epilepsy; SWM = superficial white matter

Received February 1, 2016. Revised April 21, 2016. Accepted May 31, 2016. Advance Access publication June 29, 2016

Introduction

Temporal lobe epilepsy (TLE) with mesiotemporal lobe sclerosis as its hallmark is the most common drug-resistant epilepsy in adults. MRI has been instrumental in the *in vivo* diagnosis of this lesion, which has greatly streamlined the clinical management (Cendes *et al.*, 2014). Advanced grey matter morphometry has revealed widespread atrophy beyond the temporal lobe, particularly in frontal and centro-parietal regions (Lin *et al.*, 2007; Bernhardt *et al.*, 2008, 2010; McDonald *et al.*, 2008), while diffusion MRI has shown anomalies suggestive of decreased axonal density and altered myelin membranes in deep white matter fibres (Concha *et al.*, 2005; Yogarajah *et al.*, 2009; Otte *et al.*, 2012). More recently, analysis of resting-state functional MRI has localized functional and connectional disruptions in the default mode network (Zhang *et al.*, 2010; Liao *et al.*, 2011; Pittau *et al.*, 2012; Voets *et al.*, 2012; Koepp, 2014), a set of regions comprised of lateral and medial prefrontal, parietal cortices as well as the mesiotemporal lobe (Andrews-Hanna *et al.*, 2010). These lines of evidence collectively suggest large-scale disruptions in TLE; yet, the somewhat heterogeneous distribution of findings across modalities prohibits a converging perspective on system-level pathology in this condition, likely due to a lack of studies addressing structure and function conjointly.

Given its inherent proximity to the neocortex and key role in cortico-cortical connectivity (Schüz and Braitenberg, 2002), the superficial white matter (SWM, i.e. the white matter directly beneath the cortex) is a key candidate region to evaluate the interplay between structure and function. This compartment contains both short-range association fibres that arch through cortical sulci to connect adjacent gyri as well as terminations of long-range tracts that aggregate into large fasciculi running in the depth of the white matter (Schüz and Braitenberg, 2002; Vergani *et al.*, 2014). Notably, the short association fibres make up the majority of cortico-cortical connections, with an estimated volume much larger than long-range projections (Schüz and Braitenberg, 2002). Although only few studies have examined its relationship to the adjacent cortex (Kang *et al.*, 2012; Wu *et al.*, 2014), the role of SWM is being increasingly recognized in a variety of functions such as working memory, processing speed, and visuomotor-attention (Nazeri *et al.*, 2013, 2015). Furthermore, its compromise has been associated with cognitive decline in ageing (Phillips *et al.*, 2013; Nazeri *et al.*, 2015), neuropsychiatric (Nazeri *et al.*, 2013), and neurodegenerative conditions (Miki *et al.*, 1998). Surprisingly, studies in TLE have so far neglected this region, possibly due to the focus of previous assessments on deep white matter bundles (Concha *et al.*, 2005; Yogarajah *et al.*, 2009; Otte *et al.*, 2012).

The complex fibre trajectories of the less-densely myelinated SWM challenge conventional diffusion tractography and tract-based spatial statistics, the two major techniques designed to interrogate major white matter pathways (Smith *et al.*, 2006; Oishi *et al.*, 2008; Jbabdi *et al.*, 2015; Reveley *et al.*, 2015). Our purpose was to assess the microstructural integrity of the SWM in TLE and study its relationship to large-scale structural and functional networks. We adopted a surface-based sampling approach that integrated diffusion MRI parameters with those derived from anatomical and functional MRI within a unified framework. Multivariate analysis mapped the topography of SWM diffusion anomalies between patients and controls. Statistical correlation and mediation analyses evaluated their relationship to cortical thickness and mesiotemporal volumes and local patterns of resting-state function.

Materials and methods

Subjects

We studied 61 consecutive patients referred to our hospital for the investigation of drug-resistant TLE [26 males, 18–53 years, mean ± standard deviation (SD) age = 34 ± 9 years]. No patient had a mass lesion (malformations of cortical development, tumours, or vascular malformations), traumatic brain injury, or a history of encephalitis. TLE diagnosis and lateralization of the seizure focus into left TLE ($n = 31$) and right TLE ($n = 30$) were determined by a comprehensive evaluation including detailed history, neurological examination, review of medical records, video-EEG recordings, and clinical MRI evaluation, which showed hippocampal atrophy and increased T_2 signal intensity in 37/61 (61%). Quantitative analysis including volumetry and shape modelling revealed variable degrees of ipsilateral atrophy in all patients (Bernasconi *et al.*, 2003; Bernhardt *et al.*, 2013).

The comprehensive investigation recommended TLE surgery as treatment to all patients, 43 of which underwent a selective amygdalo-hippocampectomy. Histological analysis of resected specimens (Blümcke *et al.*, 2013), available in all, revealed hippocampal sclerosis. Sixteen patients showed severe neuronal cell loss and gliosis in both CA1 and CA4 subfields [ILAE (International League Against Epilepsy) hippocampal sclerosis type 1], seven showed neuronal loss predominantly in CA1 (ILAE hippocampal sclerosis type 2), five predominantly in CA4 (ILAE hippocampal sclerosis type 3), and 15 had only gliosis without detectable neuronal loss. At a mean follow-up time of 52 ± 21 months (range: 14–88 months), 30 (70%) patients had Engel Class I outcome, 7 (16%) Class II, and 6 (14%) Class III. We observed comparable rates of seizure-free patients across ILAE hippocampal sclerosis subtypes: [type 1: 14/16 (88%), type 2: 5/7 (71%), type 3: 5/5 (100%), chi-squared: $P = 0.36$], while rates were lower in patients with isolated gliosis [6/15 (40%), chi-squared: $P = 0.01$]. Among the 18 non-operated patients, nine are currently awaiting surgery and nine delayed it for personal reasons.

The control group consisted of 38 age- and sex-matched healthy individuals (21 males; 20–53 years; mean ± SD age = 30 ± 7 years). Details on patients and controls are provided in Table 1. The Ethics Committee of the Montreal

Table 1 Demographic and clinical information

	Age	Male, *n*	Onset	Duration	FC	Surgery	Engel I
Left TLE (*n* = 31)	34 ± 9 (18–53)	11	18 ± 10 (4–40)	16 ± 10 (2–45)	7	19	13 (68%)
Right TLE (*n* = 30)	34 ± 9 (20–52)	15	14 ± 9 (1–30)	20 ± 11 (3–41)	12	24	17 (71%)
Controls (*n* = 38)	30 ± 7 (20–53)	21	NA	NA	NA	NA	NA

Age, onset, and duration are presented in mean ± SD (year, range). FC = febrile convulsions; Engel I = seizure-free, i.e. Class I postsurgical outcome in Engel's classification; NA = not applicable.

Neurological Institute and Hospital approved the study and written informed consent was obtained from all participants.

Imaging

MRI scans were acquired on a 3 T Siemens TimTrio using a 32-channel head coil (Siemens Healthcare). Our protocol consisted of 3D T_1-weighted magnetization-prepared rapid-acquisition gradient echo images (MPRAGE; repetition time = 2300 ms, echo time = 2.98 ms, inversion time = 900 ms, flip angle = 9°, voxel size = 1 × 1 × 1 mm^3, acquisition time = 5 min 30 s), 2D twice-refocused echo-planar diffusion-weighted images (repetition time = 8400 ms, echo time = 90 ms, flip angle = 90°, 63 axial slices, voxel size = 2 × 2 × 2 mm^3, diffusion-sensitized images in 64 diffusion directions with b = 1000 s/mm^2 along with one non-diffusion weighted volume, acquisition time = 9 min 33 s), and 2D echo planar resting-state functional MRI (repetition time = 2020 ms, echo time = 30 ms, flip angle = 90°, 34 axial slices, voxel size = 4 × 4 × 4 mm^3, 150 volumes, acquisition time = 5 min 9 s). For the latter, participants were instructed to keep their eyes closed while remaining awake; to minimize signal loss and distortion affecting orbitofrontal and mesiotemporal regions, slices were tilted in an oblique coronal orientation.

Image analysis

MRI preprocessing and multimodal data fusion

T_1-weighted images underwent automated correction for intensity non-uniformity (Sled *et al.*, 1998), intensity standardization, and linear registration to stereotaxic space based on the hemisphere-symmetric MNI ICBM152 template (Fonov *et al.*, 2009), and classified into white matter, grey matter, and CSF (Kim *et al.*, 2015). Diffusion-weighted MRI was analysed using FSL [version 5; www.fmrib.ox.ac.uk/fsl]. Data underwent distortion correction using 'fugue', based on a gradient echo field map acquired within the same imaging session, as well as motion and eddy current correction using 'eddy_correct'. The diffusion tensor was estimated at each voxel using 'dtifit', which also provided maps of fractional anisotropy and mean diffusivity. Resting-state functional MRI processing was based on DPARSF for Matlab (version 2.3; http://rfmri.org/DPARSF). We removed the first five volumes from each time series to ensure magnetization equilibrium, and performed slice-timing and motion correction. To correct for residual motion, image frames with a displacement exceeding 0.5 mm were regressed out from the analysis. Diffusion MRI and functional MRI were linearly registered to the corresponding T_1-weighted volumes in MNI space using a boundary-based approach that maximizes the alignment between intensity gradients of structural and echo-planar data (Greve and Fischl, 2009).

Generation of cortical and subcortical surface models

We applied the CLASP algorithm (Kim *et al.*, 2005) on preprocessed T_1-weighted data to generate models of the inner (grey matter–white matter) and outer (grey matter–CSF) surfaces with 41 000 vertices per hemisphere. CLASP iteratively warps a surface mesh to fit the white–grey matter boundary; this boundary was then expanded along a Laplacian map to model the grey matter–CSF surface. To increase across-subjects correspondence in measurement locations, surfaces were aligned to a template based on cortical folding (Lyttelton *et al.*, 2007). Surface extraction accuracy was visually verified.

To examine the SWM, we computed a Laplacian potential field between the white–grey matter interface and the ventricular walls to guide placement of a surface running 2 mm below the grey–white matter boundary (Fig 1A). This depth was chosen to target both the U-fibre system and terminations of long range bundles that lie approximately between 1.5 and 2.5 mm below the cortical interface (Schüz and Braitenberg, 2002). The Laplacian field ensured isomorphic (i.e. 1:1) mapping between points on the SWM surface and those on the overlying cortex, a necessary step to integrate grey and white matter metrics.

Feature calculation

We mapped all surfaces (i.e. grey matter–white matter, grey matter–CSF, SWM) generated on T_1-weighted MRI to the native space of each modality using the inverse transformation of the initial co-registration. Extracting features in their native space minimized data interpolation. Cortical thickness was calculated as the Euclidean distance between corresponding points on grey matter–white matter and grey matter–CSF surfaces (Kim *et al.*, 2005). We computed the amplitude of low-frequency functional fluctuations (ALFF) in the 0.01–0.08 Hz frequency band as a marker of local function. ALFF has been suggested to reveal functional changes in task-free paradigms (Zang *et al.*, 2007). Following previous recommendations (Zou *et al.*, 2008), we also assessed fractional ALFF, a normalized amplitude marker. Functional measures were sampled at the 50% intracortical surface. Diffusion parameters fractional

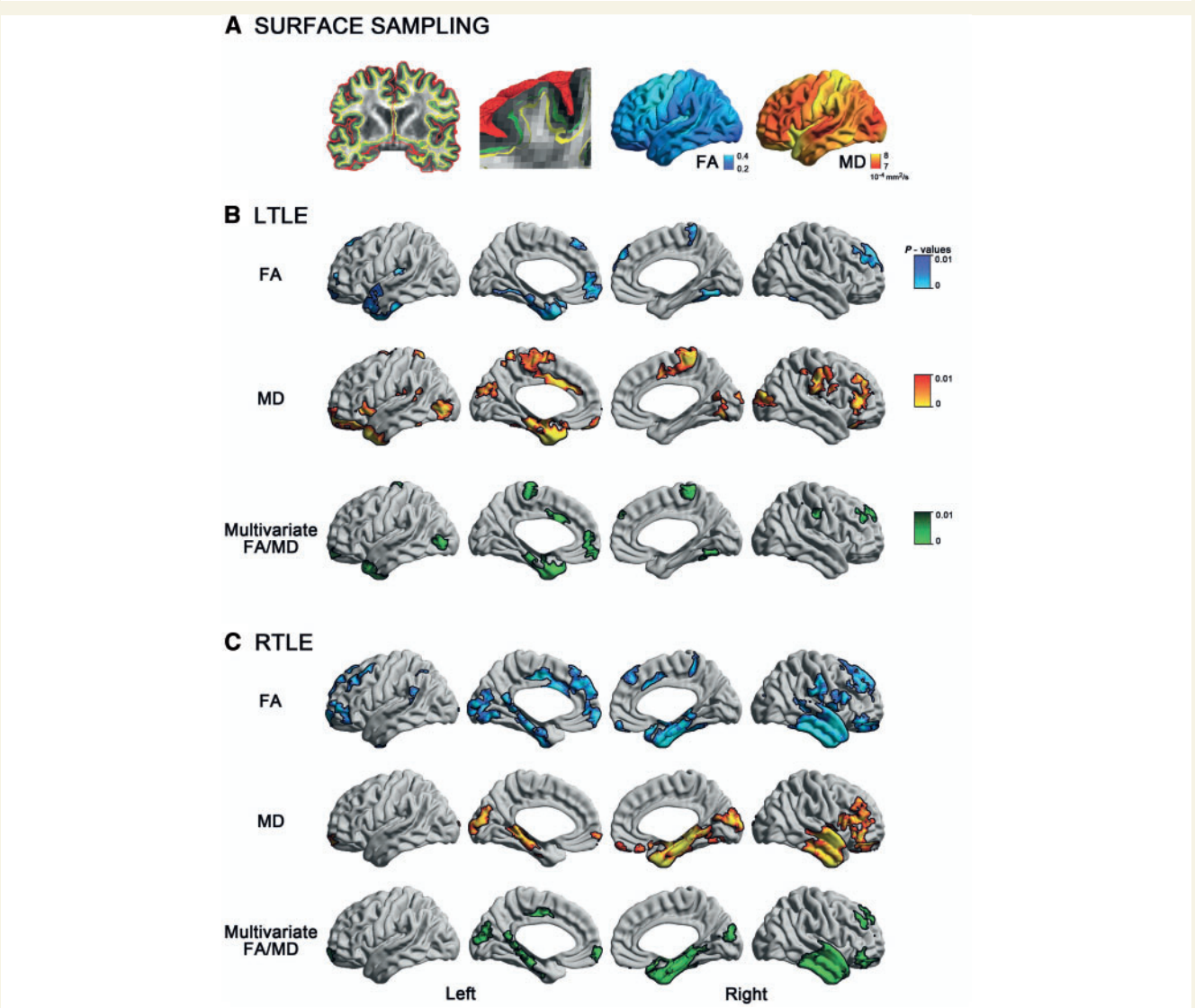

Figure 1 Surface-based mapping of SWM diffusion in TLE. (**A**) After generating the inner (white matter–grey matter, green) and outer (grey matter–CSF, red) cortical surfaces, we computed a Laplacian potential field between the white matter–grey matter interface and the ventricular walls to guide placement of a surface running 2 mm below the white matter–grey matter boundary (SWM, yellow). Fractional anisotropy (FA) and mean diffusivity (MD) were sampled on this surface. (**B**) and (**C**) show uni- and multivariate SWM diffusion anomalies in left (left TLE) and right (right TLE) patients relative to controls. To correct for multiple comparisons, findings were thresholded at $P_{FWE} < 0.05$, using random field theory for non-isotropic images (cluster threshold $P < 0.01$).

anisotropy and mean diffusivity, surrogates of fibre architecture and tissue microstructure (Beaulieu, 2002), were interpolated at the 2 mm SWM surface. The hippocampus was automatically segmented using a surface-based multi-template algorithm that has previously shown excellent accuracy in healthy individuals and patients with TLE (Kim *et al.*, 2012).

Statistical analysis

As in previous studies (Bernhardt *et al.*, 2009, 2015), analyses were carried out using SurfStat for Matlab (R2012b, The Mathworks, Natick) (Worsley *et al.*, 2009). Prior to analysis, all surface-based measurements (cortical thickness, fractional anisotropy, mean diffusivity, ALFF) were blurred using a diffusion kernel that respects surface topology, with a bandwidth of full-width at half-maximum = 20 mm, and *z*-normalized at each surface point with respect to the corresponding distribution in controls.

Mapping microstructural integrity of superficial white matter

We separately compared fractional anisotropy and mean diffusivity between each patient group (left TLE, right TLE) and controls. Multivariate Hoteling's *t*-tests assessed joint diffusion anomalies in patients. In regions of findings, we calculated Cohen's *d* effect sizes. To address possible confounds of grey matter atrophy on SWM alterations, we repeated the analysis

after statistically controlling for thickness measures at each surface point.

We assessed population-level reproducibility using bootstrap simulations (Bernhardt *et al.*, 2010), where each cohort (i.e. left TLE, right TLE, controls) was randomly resampled with replacement 1000 times. At each iteration, we performed surface-based *t*-tests between resampled left TLE/right TLE and controls and finally mapped the probabilities of observing a between-cohort difference across iterations.

Assessing the relation of superficial white matter integrity to grey matter morphology and function

We first mapped differences in cortical thickness and ALFF in patients relative to controls using surface-based *t*-tests (similar to the above analysis). We then separately evaluated spatial overlaps between thickness, ALFF, and multivariate SWM diffusion changes. Furthermore, after averaging each metric within clusters of significant findings, we performed correlation analyses between multivariate SWM diffusion changes and morphology (cortical thickness and hippocampal volume), as well as local function (ALFF). The individual load of SWM diffusion changes was summarized using the Mahalanobis distance (a multivariate z-score), calculated from the joint fractional anisotropy/mean diffusivity distribution with respect to controls and averaged within clusters of diffusion findings. Correlations were carried out in patients and controls separately; linear interaction models assessed between-group differences. We used statistical mediation analysis to further clarify the relationship between hippocampal volume, SWM changes, and ALFF (Baron and Kenny, 1986). This method tests a hypothesized causal chain in which a given 'mediator' variable affects the relationship between a predictor variable and an outcome variable. The first analysis tested effects of hippocampal volume on SWM changes, while a second analysis assessed effects of SWM alterations on ALFF. For these analyses, we combined left TLE and right TLE patients into a single cohort to increase statistical power. Prior to pooling, hemisphere-specific measures (diffusion, cortical thickness, hippocampal volume, ALFF) were z-normalized with respect to corresponding measures in controls to account for normal interhemispheric asymmetry, and sorted relative to the side of the focus.

Assessing the relationship between clinical variables and superficial white matter diffusion

In patients, we assessed the relation between multivariate SWM diffusion (i.e. the Mahalanobis distance) and history of febrile convulsions, age at seizure onset, duration of epilepsy, secondary generalization, and postoperative outcome using linear models. For these analyses, we combined left TLE and right TLE patients into a single cohort to increase statistical power and assessed overall effects in clusters of findings.

Correction for multiple comparisons

Surface-based analyses were corrected using random field theory (Worsley *et al.*, 1999), controlling the family-wise error to $P_{FWE} < 0.05$.

Results

Topography of superficial white matter diffusion anomalies

Results are shown in Fig.1. Compared to controls, both TLE groups presented with reduced fractional anisotropy and increased mean diffusivity in mesiotemporal, temporopolar, cingulate, and orbitofrontal cortices. Multivariate analysis synthesized a consistent temporo-limbic pattern of joint fractional anisotropy/mean diffusivity changes. Average *Cohen's d* effect sizes in clusters of findings were 0.63 ± 0.07 for left TLE and 0.69 ± 0.13 for right TLE. Bootstrap analysis indicated high reproducibility, with similar diffusion changes measurable in $> 75\%$ of simulations (Supplementary Fig. 1). Repeating the analysis with age as covariate and in patients with Engel I outcome revealed virtually the same findings as our main analysis using the entire cohort (Supplementary Figs 2 and 3). Directly contrasting left TLE to right TLE patients with Engel I outcome did not reveal any group difference ($P > 0.8$).

Relation of superficial white matter to grey matter structure

Three lines of evidence suggested independence between cortical thickness alterations and SWM diffusion changes: First, intersecting maps of cortical thinning in TLE with those showing SWM alterations revealed only small and scattered spatial overlaps, limited to the ipsilateral temporal pole for left TLE and ipsilateral mesiotemporal cortex for right TLE (Fig. 2). Second, in clusters of SWM findings, the degree of overall diffusion changes did not correlate with cortical thinning ($P > 0.1$). Third, comparing SWM diffusion parameters between patients and controls after correcting for thickness at each vertex did not modify results.

In relation to the hippocampus, we observed a negative correlation between volume ipsilateral to the seizure focus and clusters of SWM diffusion changes in patients ($r = -0.47$, $P < 0.0002$; Fig. 3), but not in controls ($|r| < 0.002$, $P > 0.9$). In other words, patients with more marked ipsilateral hippocampal atrophy displayed a higher load of SWM anomalies. Moreover, linear interaction analysis demonstrated a significant discrepancy in slopes between patients and controls ($t > 2.6$, $P < 0.005$), supporting that the relationship between hippocampal volume loss and SWM anomalies was specific to TLE. Finally, mediation analysis indicated that hippocampal volume significantly mediated effects of group (TLE versus controls) on SWM diffusion anomalies, where adjusting for hippocampal volume reduced the diffusion group-difference by 17% ($P < 0.05$). Interestingly, grouping patients based on histopathology showed a higher load of diffusion alterations in patients with cell loss and gliosis (ILAE hippocampal sclerosis type 1–3) compared to those with isolated gliosis ($P < 0.003$), cross-validating the

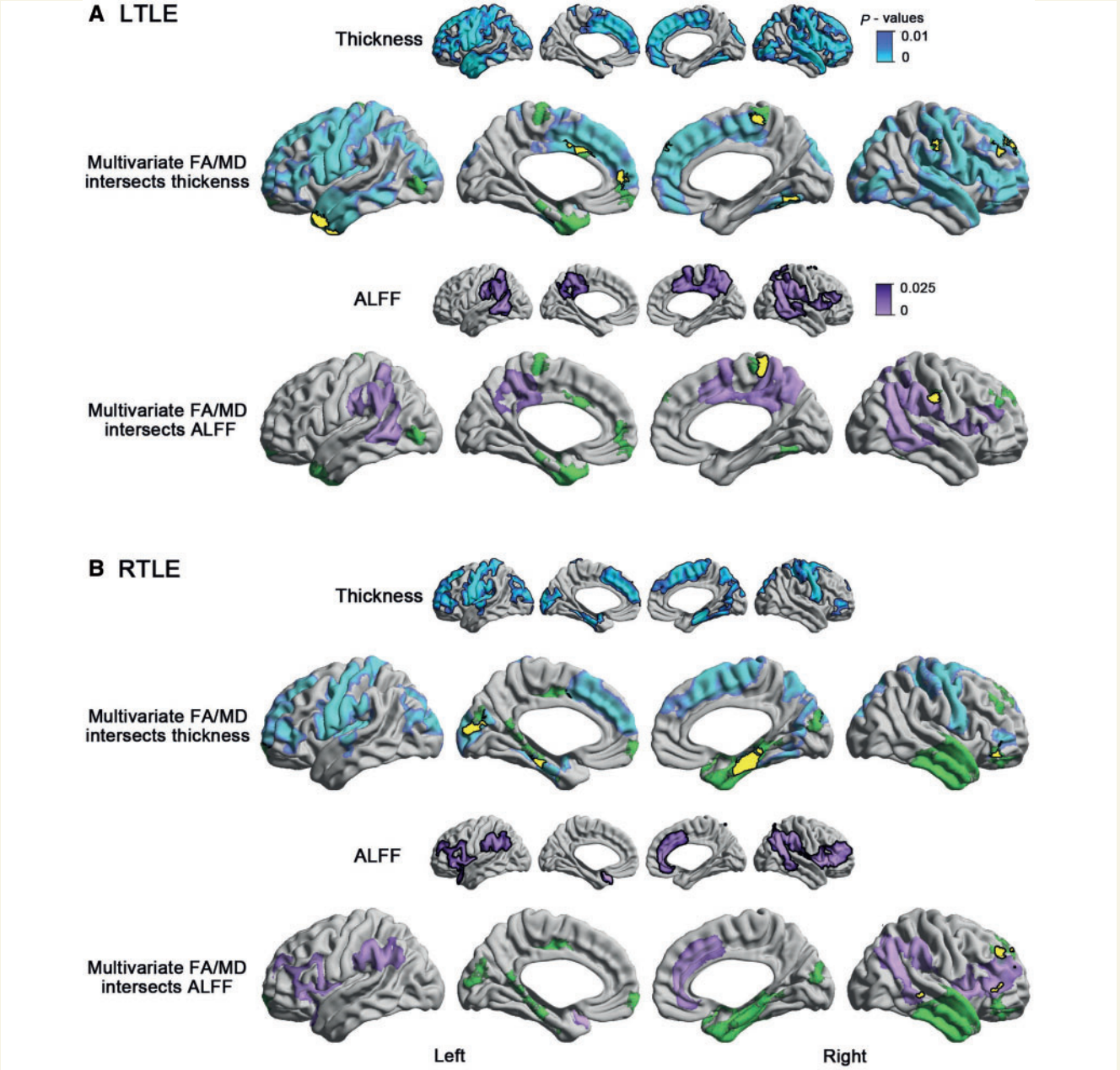

Figure 2 Spatial relationship between multivariate diffusion changes and cortical thinning as well as decrease of the resting state ALFF in left TLE (A, LTLE) and right TLE (B, RTLE) relative to controls. For a given TLE cohort, small maps show significant cortical thinning/ALFF reduction relative to controls, while yellow clusters on the multivariate maps represent the surface-based intersections between reduction in cortical thickness/ALFF and SWM changes. FA = fractional anisotropy; MD = mean diffusivity.

relationship between hippocampal damage and SWM microstructural anomalies using a direct, MRI-independent index of pathology.

Relation of superficial white matter to function

Compared to controls, patients showed decreased ALFF in bilateral precuneus, lateral frontal, temporo-parietal, and cingulate regions (Fig. 2), distinct from the distribution of SWM diffusion changes but largely overlapping with core nodes of the default mode network. A separate analysis based on previously published regions of interest (Andrews-Hanna *et al.*, 2010), as well as assessing fractional ALFF, an alternative marker of functional amplitude (Zou *et al.*, 2008) confirmed results ($P < 0.01$ and $P < 0.0001$, respectively).

We observed a negative correlation between clusters of ALFF decreases and those of diffusion abnormalities in

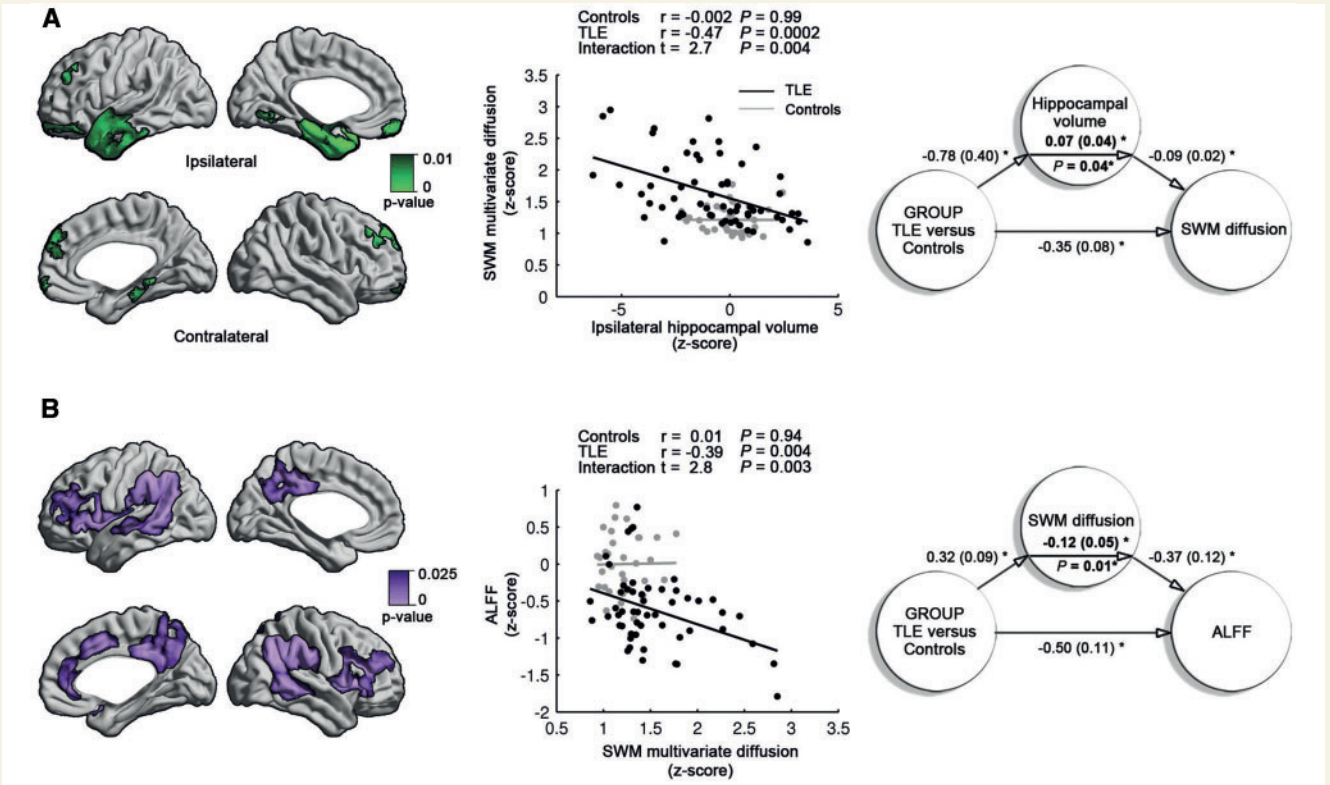

Figure 3 Relation of superficial white matter (SWM) to hippocampal volume (A) and function (B) in TLE. The maps represent the extent of SWM diffusion anomalies and amplitude of low frequency fluctuations (ALFF). Relationships and causality are shown in the correlation (*middle*) and mediation (*right*) graphs, respectively. In **A**, the degree of SWM diffusion anomalies negatively correlate with hippocampal volume ipsilateral to the focus in patients, but not controls. Hippocampal volume partially mediates SWM diffusion changes ($P = 0.04$). In **B**, decreased resting-state ALFF in patients relative to controls negatively correlates with the degree of diffusion anomalies in patients, but not controls. Moreover, diffusion anomalies mediate the abnormal function ($P = 0.01$). Numbers in mediation graphs represent path coefficients and standard errors. Asterisks denote significant coefficients with $P < 0.05$.

patients ($r = -0.39$, $P < 0.004$, Fig. 3), but not controls; interaction analysis indeed demonstrated a significant discrepancy in slopes ($t = 2.8$, $P < 0.003$). In other words, patients with more marked SWM anomalies also showed larger decreases in functional amplitude. Notably, diffusion alterations were found to mediate the effect of group (TLE versus controls) on ALFF decreases, where adjusting for SWM diffusion anomalies reduced the ALFF group difference by 19% ($P < 0.05$).

Relation of superficial white matter to clinical variables

In clusters of findings, we observed more marked diffusion anomalies in patients with a history of febrile convulsions ($t = 3.87$, $P < 0.001$), and more marked anomalies in patients with a longer duration of epilepsy ($r = 0.33$, $P = 0.01$). Similarly, anomalies were more marked in patients with earlier onset of epilepsy ($r = -0.35$, $P = 0.007$). With respect to outcome, we observed more marked diffusion alterations in patients who became completely seizure-free (Engel IA, $n = 28$) relative to those with seizure relapse after surgery (Engel IB-III; $t = 2.0$, $P = 0.05$); moreover, whole-brain comparison between outcome groups showed more marked multivariate changes in the ipsilateral lateral temporal and frontal SWM in Engel IA (Supplementary Fig. 4).

Discussion

Our novel image processing paradigm permitted continuous sampling of diffusion parameters within the superficial white matter (SWM), a region so far neglected in TLE neuroimaging studies. Distinct from previous methods based on probabilistic tractography and parameter interpolation along surface normal vectors (Kang *et al.*, 2012; Nazeri *et al.*, 2015), our approach adhered to the anatomy of overlying cortical areas through the use of a Laplacian deformation field that propagated the sampling grid into the SWM (Lui *et al.*, 2011). Notably, one of the core goals of the study being to assess the relation between SWM abnormalities and markers of hippocampal damage, we covered the spectrum of unilateral TLE by including patients with variable degrees of hippocampal

atrophy. Multivariate analysis revealed SWM diffusion alterations primarily in ipsilateral limbic regions, including parahippocampal, temporopolar, lateral temporal, anterior cingulate, and orbitofrontal regions. Anomalies were similar in left and right TLE patients and bootstrap-reproducible, suggesting population-level generalizability. While diffusion alterations occurred rather independently from cortical thinning, a battery of correlation and statistical mediation analyses suggested that they likely constitute an important link in the chain between hippocampal atrophy and large-scale functional alterations. Collectively, our findings thus suggest specificity and functional relevance of SWM alterations to pathological network reconfigurations in TLE.

Although virtually no direct MRI-histopathological correlation studies of SWM exist in TLE, histological analyses of the deep white matter in animals and patients have generally related decreased fractional anisotropy to degradation of myelin sheaths and fibre membranes, as well as decreases of fibre density, while high mean diffusivity values are thought to be due to increases of extra-axonal space together with reactive astrogliosis (Beaulieu, 2002; Concha *et al.*, 2010; van Eijsden *et al.*, 2011). Notably, there have been reports of astrocytic and microcytic gliosis in the white matter adjacent to the gyral crowns (Blanc *et al.*, 2011); however, the integrity of axon and myelin in these regions has not been examined. Our findings of co-localized fractional anisotropy and mean diffusivity alterations could thus reflect a complex pathological process in the SWM that combines axonal and gliotic components.

In line with previous observations (Bernhardt *et al.*, 2009, 2010; Coan *et al.*, 2009), cortical thinning was bilaterally distributed in frontal and centro-parietal regions. Conversely, SWM anomalies followed mainly a temporo-limbic topography with minimal overlap with cortical thinning. In addition to their spatial divergence, the lack of correlation between thinning and diffusion changes, on the one hand, and the robustness of group-level SWM findings after correcting for corresponding thickness measures, on the other hand, further support dissociation. Altogether, these observations imply independent pathological processes affecting the temporo-limbic SWM and grey matter morphology. While cortical thinning may stem from the effects of seizure spread through thalamocortical pathways (Bernhardt *et al.*, 2012), SWM alterations likely relate to hippocampal damage. Indeed, our study showed that besides correlating with hippocampal volume, SWM anomalies were partially mediated by hippocampal atrophy, a finding cross-validated by higher load of diffusion anomalies in patients with cell loss and gliosis (ILAE hippocampal sclerosis types 1–3) compared to those with isolated gliosis (ILAE hippocampal sclerosis type 4). Moreover, a moderate correlation with history of febrile convulsion bears resemblance with previous results focusing on the hippocampus alone (Cendes *et al.*, 1993; Davies *et al.*, 1996; Barr *et al.*, 1997; Düzel *et al.*, 2004), further suggesting that SWM anomalies may likely undergo similar pathological processes as the mesiotemporal region. Notably, the proximity of SWM findings to the mesiotemporal lobe and close relationship to hippocampal pathology may corroborate connectivity-based models of regional susceptibility in disease, in which regions anatomically connected to a pathological epicentre may undergo most marked structural alterations (Fornito *et al.*, 2015), while pathological burden, at least at the level of the white matter, may taper off with increasing distance from the core (Concha *et al.*, 2012).

Emerging studies have suggested that TLE is associated with large-scale functional alterations. In particular, recent resting-state functional MRI investigations have highlighted anomalies predominantly in regions forming the default mode network (Frings *et al.*, 2009; Zhang *et al.*, 2010; Liao *et al.*, 2011; Voets *et al.*, 2012), an assembly thought to play a key role in internally generated cognition, memory, and future planning (Andrews-Hanna *et al.*, 2014). Given the well-established relation between TLE and hippocampal damage, default mode network anomalies found in our study are in concordance with theories linking functional processes mediated by this network to the hippocampus and its efferent connectivity system (Buckner *et al.*, 2008). Moreover, regionally unconstrained mapping of functional amplitude, a marker associated to local bulk activation (Zhang *et al.*, 2010), confirmed functional decreases in TLE relative to controls primarily in posterior default mode nodes, such as the precuneus, retrosplenial cortex, and lateral temporo-parietal regions. In accordance to our findings, previous resting-state functional MRI studies in TLE have also reported abnormal interactions between mesiotemporal seeds and default mode components (Frings *et al.*, 2009; Pittau *et al.*, 2012; Doucet *et al.*, 2013; James *et al.*, 2013; Haneef *et al.*, 2014; Bernhardt *et al.*, 2016). Functional disruptions in the default mode could, in turn, be explained in view of the central role the hippocampus plays in this intrinsic functional network (Buckner *et al.*, 2008), with potential consequences on the reorganization of memory circuits. In particular, a recent functional connectivity analysis during a working memory task has suggested that hippocampal damage may ultimately affect the segregation/integration of the default mode network with other functional networks, thus potentially modulating the dynamic interplay between both task-positive and -negative networks (Stretton *et al.*, 2013; Sidhu *et al.*, 2015). Importantly, we showed that SWM damage (itself mediated by hippocampal atrophy) resulted in large-scale default mode anomalies, a link that needs to be targeted by future longitudinal studies in new onset epilepsies and ideally complemented by extensive behavioural phenotyping to understand the cognitive consequences of this causal chain (Witt and Helmstaedter, 2015). In addition, serial investigations that include both pre- and postoperative imaging may offer a window into the causal consequences of mesiotemporal resections on the SWM changes, and may furthermore be used to address downstream effects on memory network organization (Sidhu *et al.*, 2015).

Funding

This work was supported by the Canadian Institutes of Health Research (CIHR MOP-57840 and CIHR MOP-123520). BCB and ML received fellowships from CIHR and Savoy Foundation for Epilepsy, respectively.

Supplementary material

Supplementary material is available at *Brain* online.

References

Andrews-Hanna JR, Reidler JS, Sepulcre J, Poulin R, Buckner RL. Functional-anatomic fractionation of the brain's default network. Neuron 2010; 65: 550–62.

Andrews-Hanna JR, Smallwood J, Spreng RN. The default network and self-generated thought: component processes, dynamic control, and clinical relevance. Ann NY Acad Sci 2014; 1316: 29–52.

Baron RM, Kenny DA. The moderator-mediator variable distinction in social psychological research: conceptual, strategic, and statistical considerations. J Pers Soc Psychol 1986; 51: 1173–82.

Barr WB, Ashtari M, Schaul N. Bilateral reductions in hippocampal volume in adults with epilepsy and a history of febrile seizures. J Neurol Neurosurg Psychiatry 1997; 63: 461–7.

Beaulieu C. The basis of anisotropic water diffusion in the nervous system—a technical review. NMR Biomed 2002; 15: 435–55.

Bernasconi N, Bernasconi A, Caramanos Z, Antel SB, Andermann F, Arnold DL. Mesial temporal damage in temporal lobe epilepsy: a volumetric MRI study of the hippocampus, amygdala and parahippocampal region. Brain 2003; 126: 462–9.

Bernhardt BC, Bernasconi N, Concha L, Bernasconi A. Cortical thickness analysis in temporal lobe epilepsy: reproducibility and relation to outcome. Neurology 2010; 74: 1776–84.

Bernhardt BC, Bernasconi N, Kim H, Bernasconi A. Mapping thalamocortical network pathology in temporal lobe epilepsy. Neurology 2012; 78: 129–36.

Bernhardt BC, Bernasconi A, Liu M, Hong SJ, Caldairou B, Goubran M, et al. The spectrum of structural and functional imaging abnormalities in temporal lobe epilepsy. Ann Neurol 2016; 80: 142–53.

Bernhardt BC, Hong S, Bernasconi A, Bernasconi N. Magnetic resonance imaging pattern learning in temporal lobe epilepsy: classification and prognostics. Ann Neurol 2015; 77: 436–46.

Bernhardt BC, Kim H, Bernasconi N. Patterns of subregional mesiotemporal disease progression in temporal lobe epilepsy. Neurology 2013; 81: 1840–7.

Bernhardt BC, Worsley KJ, Besson P, Concha L, Lerch JP, Evans AC, et al. Mapping limbic network organization in temporal lobe epilepsy using morphometric correlations: insights on the relation between mesiotemporal connectivity and cortical atrophy. Neuroimage 2008; 42: 515–24.

Bernhardt BC, Worsley KJ, Kim H, Evans AC, Bernasconi A, Bernasconi N. Longitudinal and cross-sectional analysis of atrophy in pharmacoresistant temporal lobe epilepsy. Neurology 2009; 72: 1747–54.

Blanc F, Martinian L, Liagkouras I, Catarino C, Sisodiya SM, Thom M. Investigation of widespread neocortical pathology associated with hippocampal sclerosis in epilepsy: a postmortem study. Epilepsia 2011; 52: 10–21.

Blümcke I, Thom M, Aronica E, Armstrong DD, Bartolomei F, Bernasconi A, et al. International consensus classification of hippocampal sclerosis in temporal lobe epilepsy: a task force report from the ILAE commission on diagnostic methods. Epilepsia 2013; 54: 1315–29.

Buckner RL, Andrews-Hanna JR, Schacter DL. The brain's default network: anatomy, function, and relevance to disease. Ann NY Acad Sci 2008; 1124: 1–38.

Cendes F, Andermann F, Gloor P, Lopes-Cendes I, Andermann E, Melanson D, et al. Atrophy of mesial structures in patients with temporal lobe epilepsy: cause or consequence of repeated seizures? Ann Neurol 1993; 34: 795–801.

Cendes F, Sakamoto AC, Spreafico R, Bingaman W, Becker AJ. Epilepsies associated with hippocampal sclerosis. Acta Neuropathol 2014; 128: 21–37.

Coan AC, Appenzeller S, Bonilha L, Li LM, Cendes F. Seizure frequency and lateralization affect progression of atrophy in temporal lobe epilepsy. Neurology 2009; 73: 834–42.

Concha L, Beaulieu C, Gross DW. Bilateral limbic diffusion abnormalities in unilateral temporal lobe epilepsy. Ann Neurol 2005; 57: 188–96.

Concha L, Kim H, Bernasconi A, Bernhardt BC, Bernasconi N. Spatial patterns of water diffusion along white matter tracts in temporal lobe epilepsy. Neurology 2012; 79: 455–62.

Concha L, Livy DJ, Beaulieu C, Wheatley BM, Gross DW. *In vivo* diffusion tensor imaging and histopathology of the fimbria-fornix in temporal lobe epilepsy. J Neurosci 2010; 30: 996–1002.

Davies KG, Hermann BP, Dohan FC, Foley KT, Bush AJ, Wyler AR. Relationship of hippocampal sclerosis to duration and age of onset of epilepsy, and childhood febrile seizures in temporal lobectomy patients. Epilepsy Res 1996; 24: 119–26.

Doucet G, Osipowicz K, Sharan A, Sperling MR, Tracy JI. Hippocampal functional connectivity patterns during spatial working memory differ in right versus left temporal lobe epilepsy. Brain Connect 2013; 3: 398–406.

Düzel E, Kaufmann J, Guderian S, Szentkuti A, Schott B, Bodammer N, et al. Measures of hippocampal volumes, diffusion and 1H MRS metabolic abnormalities in temporal lobe epilepsy provide partially complementary information. Eur J Neurol 2004; 11: 195–205.

Fonov V, Evans A, McKinstry R, Almli C, Collins D. Unbiased nonlinear average age-appropriate brain templates from birth to adulthood. Neuroimage 2009; 47: S102.

Fornito A, Zalesky A, Breakspear M. The connectomics of brain disorders. Nat Rev Neurosci 2015; 16: 159–72.

Frings L, Schulze-Bonhage A, Spreer J, Wagner K. Remote effects of hippocampal damage on default network connectivity in the human brain. J Neurol 2009; 256: 2021–9.

Greve DN, Fischl B. Accurate and robust brain image alignment using boundary-based registration. Neuroimage 2009; 48: 63–72.

Haneef Z, Lenartowicz A, Yeh HJ, Levin HS, Engel J, Stern JM. Functional connectivity of hippocampal networks in temporal lobe epilepsy. Epilepsia 2014; 55: 137–45.

James GA, Tripathi SP, Ojemann JG, Gross RE, Drane DL. Diminished default mode network recruitment of the hippocampus and parahippocampus in temporal lobe epilepsy. J Neurosurg 2013; 119: 288–300.

Jbabdi S, Sotiropoulos SN, Haber SN, Essen DC Van, Behrens TE. Measuring macroscopic brain connections in vivo. Nat Neurosci 2015; 18: 1546–55.

Kang X, Herron TJ, Turken AU, Woods DL. Diffusion properties of cortical and pericortical tissue: regional variations, reliability and methodological issues. Magn Reson Imaging 2012; 30: 1111–22.

Kim H, Caldairou B, Hwang J-W, Mansi T, Hong S-J, Bernasconi N, et al. Accurate cortical tissue classification on MRI by modeling cortical folding patterns. Hum Brain Mapp 2015; 36: 3563–74.

Kim H, Chupin M, Colliot O, Bernhardt BC, Bernasconi N, Bernasconi A. Automatic hippocampal segmentation in temporal lobe epilepsy: impact of developmental abnormalities. Neuroimage 2012; 59: 3178–86.

Kim JS, Singh V, Lee JK, Lerch J, Ad-Dab'bagh Y, MacDonald D, et al. Automated 3-D extraction and evaluation of the inner and

outer cortical surfaces using a laplacian map and partial volume effect classification. Neuroimage 2005; 27: 210–21.
Koepp MJ. Neuroimaging of drug resistance in epilepsy. Curr Opin Neurol 2014; 27: 192–8.
Liao W, Zhang Z, Pan Z, Mantini D, Ding J, Duan X, et al. Default mode network abnormalities in mesial temporal lobe epilepsy: a study combining fMRI and DTI. Hum Brain Mapp 2011; 32: 883–95.
Lin JJ, Salamon N, Lee AD, Dutton RA, Geaga JA, Hayashi KM, et al. Reduced neocortical thickness and complexity mapped in mesial temporal lobe epilepsy with hippocampal sclerosis. Cereb Cortex 2007; 17: 2007–18.
Lui JH, Hansen DV, Kriegstein AR. Development and evolution of the human neocortex. Cell 2011; 146: 18–36.
Lyttelton O, Boucher M, Robbins S, Evans A. An unbiased iterative group registration template for cortical surface analysis. Neuroimage 2007; 34: 1535–44.
McDonald CR, Hagler Jr. DJ, Ahmadi ME, Tecoma E, Iragui V, Gharapetian L, et al. Regional neocortical thinning in mesial temporal lobe epilepsy. Epilepsia 2008; 49: 794–803.
Miki Y, Grossman RI, Udupa JK, Wei L, Kolson DL, Mannon LJ, et al. Isolated U-fiber involvement in MS: preliminary observations. Neurology 1998; 50: 1301–6.
Nazeri A, Chakravarty MM, Felsky D, Lobaugh NJ, Rajji TK, Mulsant BH, et al. Alterations of superficial white matter in schizophrenia and relationship to cognitive performance. Neuropsychopharmacology 2013; 38: 1954–62.
Nazeri A, Chakravarty MM, Rajji TK, Felsky D, Rotenberg DJ, Mason M, et al. Superficial white matter as a novel substrate of age-related cognitive decline. Neurobiol Aging 2015; 36: 2094–106.
Oishi K, Zilles K, Amunts K, Faria A, Jiang H, Li X, et al. Human brain white matter atlas: identification and assignment of common anatomical structures in superficial white matter. Neuroimage 2008; 43: 447–57.
Otte WM, van Eijsden P, Sander JW, Duncan JS, Dijkhuizen RM, Braun KPJ. A meta-analysis of white matter changes in temporal lobe epilepsy as studied with diffusion tensor imaging. Epilepsia 2012; 53: 659–67.
Phillips OR, Clark KA, Luders E, Azhir R, Joshi SH, Woods RP, et al. Superficial white matter: effects of age, sex, and hemisphere. Brain Connect 2013; 3: 146–59.
Pittau F, Grova C, Moeller F, Dubeau F, Gotman J. Patterns of altered functional connectivity in mesial temporal lobe epilepsy. Epilepsia 2012; 53: 1013–23.
Reveley C, Seth AK, Pierpaoli C, Silva AC, Yu D, Saunders RC, et al. Superficial white matter fiber systems impede detection of long-range cortical connections in diffusion MR tractography. Proc Natl Acad Sci USA 2015; 112: E2820–8.
Schüz A, Braitenberg V. The human cortical white matter: quantitative aspects of cortico-cortical long-range connectivity. Cortical Areas Unity Divers 2002: 377–84.
Sidhu MK, Stretton J, Winston GP, Symms M, Thompson PJ, Koepp MJ, et al. Memory fMRI predicts verbal memory decline after anterior temporal lobe resection. Neurology 2015; 84: 1512–19.
Sled JG, Zijdenbos AP, Evans AC. A nonparametric method for automatic correction of intensity nonuniformity in MRI data. IEEE Trans Med Imaging 1998; 17: 87–97.
Smith SM, Jenkinson M, Johansen-Berg H, Rueckert D, Nichols TE, Mackay CE, et al. Tract-based spatial statistics: voxelwise analysis of multi-subject diffusion data. Neuroimage 2006; 31: 1487–505.
Stretton J, Winston GP, Sidhu M, Bonelli S, Centeno M, Vollmar C, et al. Disrupted segregation of working memory networks in temporal lobe epilepsy. NeuroImage Clin 2013; 2: 273–81.
van Eijsden P, Otte WM, van der Hel WS, van Nieuwenhuizen O, Dijkhuizen RM, de Graaf R a, et al. In vivo diffusion tensor imaging and ex vivo histologic characterization of white matter pathology in a post-status epilepticus model of temporal lobe epilepsy. Epilepsia 2011; 52: 841–5.
Vergani F, Mahmood S, Morris CM, Mitchell P, Forkel SJ. Intralobar fibres of the occipital lobe: a post mortem dissection study. Cortex 2014; 56: 145–56.
Voets NL, Beckmann CF, Cole DM, Hong S, Bernasconi A, Bernasconi N. Structural substrates for resting network disruption in temporal lobe epilepsy. Brain 2012; 135: 2350–7.
Witt JA, Helmstaedter C. Cognition in the early stages of adult epilepsy. Seizure 2015; 26: 65–8.
Worsley K, Taylor J, Carbonell F, Chung M, Duerden E, Bernhardt B, et al. SurfStat: a matlab toolbox for the statistical analysis of univariate and multivariate surface and volumetric data using linear mixed effects models and random field theory. Neuroimage 2009; 47: S102.
Worsley KJ, Andermann M, Koulis T, MacDonald D, Evans AC. Detecting changes in nonisotropic images. Hum Brain Mapp 1999; 8: 98–101.
Wu M, Lu LH, Lowes A, Yang S, Passarotti AM, Zhou XJ, et al. Development of superficial white matter and its structural interplay with cortical gray matter in children and adolescents. Hum Brain Mapp 2014; 35: 2806–16.
Yogarajah M, Focke NK, Bonelli S, Cercignani M, Acheson J, Parker GJM, et al. Defining Meyer's loop-temporal lobe resections, visual field deficits and diffusion tensor tractography. Brain 2009; 132: 1656–68.
Zang Y-F, He Y, Zhu C-Z, Cao Q-J, Sui M-Q, Liang M, et al. Altered baseline brain activity in children with ADHD revealed by resting-state functional MRI. Brain Dev 2007; 29: 83–91.
Zhang Z, Lu G, Zhong Y, Tan Q, Chen H, Liao W, et al. fMRI study of mesial temporal lobe epilepsy using amplitude of low-frequency fluctuation analysis. Hum Brain Mapp 2010; 31: 1851–61.
Zou QH, Zhu CZ, Yang Y, Zuo XN, Long XY, Cao QJ, et al. An improved approach to detection of amplitude of low-frequency fluctuation (ALFF) for resting-state fMRI: fractional ALFF. J Neurosci Methods 2008; 172: 137–41.